

**Vector-based model of elastic bonds for simulation of granular solids**

Vitaly A. Kuzkin\* and Igor E. Asonov†

*Institute for Problems in Mechanical Engineering RAS, Saint Petersburg State Polytechnical University, St. Petersburg, Russia*

(Received 17 February 2012; revised manuscript received 31 July 2012; published xxxxx)

A model (further referred to as the V model) for the simulation of granular solids, such as rocks, ceramics, concrete, nanocomposites, and agglomerates, composed of bonded particles (rigid bodies), is proposed. It is assumed that the bonds, usually representing some additional glue-like material connecting particles, cause both forces and torques acting on the particles. Vectors rigidly connected with the particles are used to describe the deformation of a single bond. The expression for potential energy of the bond and corresponding expressions for forces and torques are derived. Formulas connecting parameters of the model with longitudinal, shear, bending, and torsional stiffnesses of the bond are obtained. It is shown that the model makes it possible to describe *any* values of the bond stiffnesses *exactly*; that is, the model is applicable for the bonds with arbitrary length/thickness ratio. Two different calibration procedures depending on bond length/thickness ratio are proposed. It is shown that parameters of the model can be chosen so that under small deformations the bond is equivalent to either a Bernoulli-Euler beam or a Timoshenko beam or short cylinder connecting particles. Simple analytical expressions, relating parameters of the V model with geometrical and mechanical characteristics of the bond, are derived. Two simple examples of computer simulation of thin granular structures using the V model are given.

DOI: [10.1103/PhysRevE.00.001300](https://doi.org/10.1103/PhysRevE.00.001300)

PACS number(s): 81.05.Rm, 45.70.-n, 45.20.da, 45.10.-b

**I. INTRODUCTION**

The discrete (or distinct) element method (DEM) [1] is widely used for the computer simulation of solid and free-flowing granular materials. Similarly to classical molecular dynamics [2,3], in the framework of DEM the material is represented by a set of many interacting rigid body particles (granules). The equations of the particles' motion are integrated numerically. In free-flowing materials the particles interact *via* contact forces, dry and viscous friction forces, electrostatic forces, etc. Computer simulation of deformation and fracture of granular solids, such as rocks [4], concrete [5], ceramics [6,7], particle compounds [8], agglomerates [9], nanocomposites [10], etc., is even more challenging. Particles in granular solids are usually connected together by some additional bonding material such as cement [4,5] or glue [6–10]. The example of composite material consisting of PbS nanoparticles bonded together by a copolymer is shown in Fig. 1 (for details, see Ref. [10]). The copolymer (bonding material) resists the relative translation and rotation of neighboring PbS particles. In DEM simulations bonding material is usually taken into account implicitly using the concept of so-called bonds [4,7,9,11]. Neighboring particles are connected by the bonds that resist stretching/compression, shear, bending, and torsion. The bonds cause forces and torques acting on the particles along with contact forces [12]. The mass of the bonding material is usually neglected [4,7,9,11]. The assumption does not influence static properties of the granular material. The influence on the dynamic properties is not so straightforward and should be considered separately. However, let us note that in many practical applications [4,7,9,10] the mass of bonding material is much smaller than the mass of the particles (see, for example, Fig. 1). Therefore, the mass of bonding material can be neglected.

According to the review, presented in Ref. [11], only a few models proposed in the literature allow a description of all possible deformations of the bond accurately. The bonded-particle model (BPM), proposed in Ref. [4], is widely used for simulation of deformation and fracture of solids, in particular, rocks [13,14] and agglomerates [9]. For example, the impact of a granule with a rigid wall is considered in Ref. [9]. Several drawbacks of the BPM, in particular, in the case of coexistence of bending and torsion of the bond, are discussed in Ref. [11]. It is noted that the main reason for the drawbacks is the incremental algorithm, used in the framework of the BPM. Also it should be noted that the BPM contains only two independent parameters, describing bond stiffnesses, while, in general, the bond has four independent stiffnesses (longitudinal, shear, bending, and torsional). A Timoshenko beam connecting particles' centers is used as a model of a bond in Ref. [15]. The model has a clear physical meaning and is applicable for thin, long bonds under small deformations. However, it has low accuracy for the description of short bonds, connecting particles' surfaces. For example, the model [15] is not accurate in the case shown in Fig. 1. Also the generalization of the model for the case of large nonlinear deformations of the bond is not straightforward. The approach, based on decomposition of relative rotation of particles, is proposed in Ref. [11]. Forces and torques are represented as functions of angles, describing the relative rotation of the particles. It is shown that the method in Ref. [11] is more accurate from the computational point of view than the incremental procedure of the BPM. Though the formalism proposed in Ref. [11] is correct from a mathematical point of view, it has a drawback. It is evident from the paper that if particles rotate in the same direction and there is no relative translation, then forces and torques are equal to zero. The reason is that the forces and torques, proposed in Ref. [11], depend only on relative position and orientation of the particles, while, in general, the dependence on the orientation of the particles with respect to the bond should also be taken into account.

\*kuzkinva@gmail.com

†Igor.asonov@gmail.com

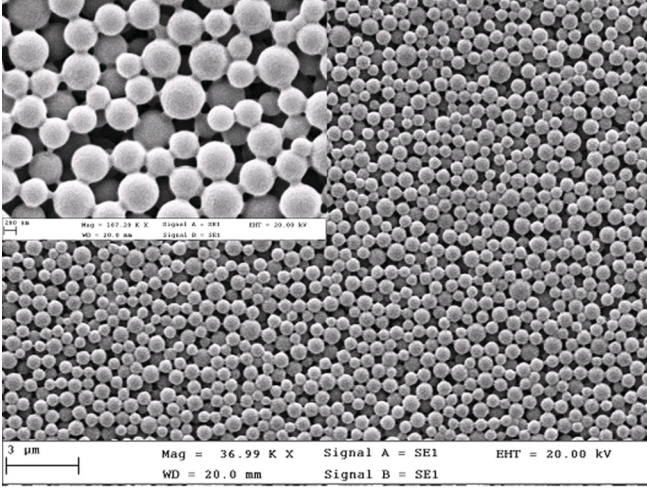


FIG. 1. Scanning electron microscope images of composite consisting of PbS nanoparticles bonded by a copolymer. From Ref. [10].

relative position, relative orientation, and orientation with respect to the vector connecting the particles. Let us introduce the following designations:  $\mathbf{F}_{ij}$  and  $\mathbf{M}_{ij}$  are force and torque, respectively, acting on particle  $i$  from particle  $j$ . Torque  $\mathbf{M}_{ij}$  is calculated with respect to the center of mass of particle  $i$ . In Ref. [17] it is shown that  $\mathbf{F}_{ij}$  and  $\mathbf{M}_{ij}$  satisfy Newton's third law, its analog for torques, and equation of energy balance,

$$\begin{aligned} \mathbf{F}_{ij} &= -\mathbf{F}_{ji}, \quad \mathbf{M}_{ij} + \mathbf{M}_{ji} - \mathbf{r}_{ij} \times \mathbf{F}_{ij} = 0, \\ \dot{U}_{ij} &= \mathbf{F}_{ij} \cdot \dot{\mathbf{r}}_{ij} - \mathbf{M}_{ij} \cdot \boldsymbol{\omega}_i - \mathbf{M}_{ji} \cdot \boldsymbol{\omega}_j, \end{aligned} \quad (1)$$

where  $\mathbf{r}_{ij} \stackrel{\text{def}}{=} \mathbf{r}_j - \mathbf{r}_i$ ;  $\mathbf{r}_i, \mathbf{r}_j$  are radius vectors of particles  $i$  and  $j$ ;  $\boldsymbol{\omega}_i, \boldsymbol{\omega}_j$  are angular velocities;  $U_{ij}$  is the internal energy of the system.

Assume that the interactions between particles are potential and that the internal energy  $U_{ij}$  depends on particles' relative position, relative orientation, and orientation with respect to  $\mathbf{r}_{ij}$ . Relative position of the particles can be described by vector  $\mathbf{r}_{ij}$ . Therefore,  $U_{ij}$  should be a function of  $\mathbf{r}_{ij}$ . In order to introduce the dependence of  $U_{ij}$  on particles' orientation the approach, initially proposed for liquids in Ref. [18] and applied for solids in Ref. [20], is used. Let us describe the orientation of particle  $i$  via the set of vectors  $\{\mathbf{n}_i^k\}_{k \in \Lambda_i}$ , rigidly connected with the particle, where  $\Lambda_i$  is a set of indexes. Hereinafter the lower index corresponds to a particle's number, while the upper index corresponds to a vector's number. The maximum amount of vectors is not limited and does not influence the general considerations. Since orientations of the particles are determined by vectors  $\{\mathbf{n}_i^k\}_{k \in \Lambda_i}$ ,  $\{\mathbf{n}_j^m\}_{m \in \Lambda_j}$ , it follows that internal energy has the form

$$U_{ij} = U(\mathbf{r}_{ij}, \{\mathbf{n}_i^k\}_{k \in \Lambda_i}, \{\mathbf{n}_j^m\}_{m \in \Lambda_j}). \quad (2)$$

Let us derive the relation between forces, torques, and potential energy  $U_{ij}$ . Substituting formula (2) into equation of energy balance (1) and assuming that forces  $\mathbf{F}_{ij}$  and torques  $\mathbf{M}_{ij}$  are independent on linear and angular velocities of the particles, one can show that

$$\begin{aligned} \mathbf{F}_{ij} &= -\mathbf{F}_{ji} = \frac{\partial U}{\partial \mathbf{r}_{ij}}, \quad \mathbf{M}_{ij} = \sum_{k \in \Lambda_i} \frac{\partial U}{\partial \mathbf{n}_i^k} \times \mathbf{n}_i^k, \\ \mathbf{M}_{ji} &= \sum_{m \in \Lambda_j} \frac{\partial U}{\partial \mathbf{n}_j^m} \times \mathbf{n}_j^m. \end{aligned} \quad (3)$$

If the internal energy (2) is known, then forces and torques are calculated using formulas (3). Note that function  $U$  must satisfy the material objectivity principle. That is, it must be invariant with respect to rigid body rotation. If the objectivity principle is satisfied, then forces and torques, calculated using formulas (3), satisfy Newton's third law for torques automatically. Therefore,  $U$  must be a function of some invariant arguments. For instance, the following invariant values can be used:  $r_{ij}, \mathbf{e}_{ij} \cdot \mathbf{n}_i^k, \mathbf{e}_{ji} \cdot \mathbf{n}_j^m, \mathbf{n}_i^k \cdot \mathbf{n}_j^m, |\mathbf{e}_{ij} \times \mathbf{n}_i^k|, |\mathbf{n}_i^k \times \mathbf{n}_j^m|$ , etc., where  $\mathbf{e}_{ij} \stackrel{\text{def}}{=} \mathbf{r}_{ij}/r_{ij}, k \in \Lambda_i, m \in \Lambda_j$ . In practice the first four expressions from the list are sufficient as the remaining invariants can be represented via their combination. These expressions have simple geometrical meaning. The first one is a distance between the particles. The second and the third invariants ( $\mathbf{e}_{ij} \cdot \mathbf{n}_i^k$  and  $\mathbf{e}_{ji} \cdot \mathbf{n}_j^m$ ) describe the orientation of particles  $i$  and  $j$  with respect to vector  $\mathbf{r}_{ij}$ . The fourth invariants

Another approach for description of interactions between both material points [2] and rigid bodies [3] is used in classical molecular dynamics. Forces and torques, acting between particles, are derived from the potential energy. Linear interactions between rigid body particles in crystalline solids are discussed in detail in Refs. [16,17]. Different types of nonlinear interactions are proposed in Refs. [3,18] and [19,20] for molecular liquids and crystalline solids, respectively.

In the present paper a vector-based model (further referred to as the V model) of elastic bonds in solids is developed using a combination of approaches, proposed in Refs. [16] and [3,18]. Equations describing interactions between two rigid bodies in the general case are summarized. The general expression for the potential energy of the bond is represented via vectors rigidly connected with bonded particles. The vectors are used for description of different types of bond deformation. The expression for potential energy corresponding to tension/compression, shear, bending, and torsion of the bond is proposed. Forces and torques acting between particles are derived from the potential energy. Two approaches for calibration of V model parameters for bonds with different length/thickness ratios are presented. Simple analytical formulas connecting geometrical and elastic characteristics of the bond with parameters of the V model are derived. The main aspects of numerical implementation of the model are discussed. Two examples of computer simulations using the V model are given.

## II. PAIR POTENTIAL INTERACTIONS BETWEEN RIGID BODIES: THE GENERAL CASE

Let us consider the approach for the description of pair potential interactions between rigid bodies in the general case [3,17,18]. In the literature the formalism is referred to as moment interactions [16,17,19–21]. In the present paper moment interactions are applied for description of elastic bonds between particles in granular solids.

Consider a system consisting of two interacting rigid body particles, marked by indexes  $i$  and  $j$ . In the general case particles interact via forces and torques depending on their

176  $\mathbf{n}_i^k \cdot \mathbf{n}_j^m$  describe the relative orientation of the particle. Thus,  
 177 in the general case the potential of interaction between rigid  
 178 bodies is represented in the following form:

$$U_{ij} = U(r_{ij}, \{\mathbf{e}_{ij} \cdot \mathbf{n}_i^k\}_{k \in \Lambda_i}, \{\mathbf{e}_{ji} \cdot \mathbf{n}_j^m\}_{m \in \Lambda_j}, \{\mathbf{n}_i^k \cdot \mathbf{n}_j^m\}_{k \in \Lambda_i, m \in \Lambda_j}). \quad (4)$$

179 In general, sets  $\Lambda_i, \Lambda_j$  may contain any number of vectors.  
 180 However, from computational point of view it is desirable to  
 181 minimize this number.

### 182 III. VECTOR-BASED MODEL OF A SINGLE BOND

183 Let us use moment interactions for the description of the  
 184 elastic deformation of the bond. Note that, in general, the  
 185 particle can be bonded with any number of neighbors. How-  
 186 ever, the behavior of the bonds is assumed to be independent.  
 187 Therefore, for simplicity, only two bonded particles  $i$  and  $j$   
 188 are considered. Assume that the bond connects two points that  
 189 belong to the particles. The points lie on the line connecting  
 190 the particles' centers in the initial (undeformed) state. For  
 191 example, the points can coincide with particles centers. Let  
 192 us denote distance from the points to the particles' centers of  
 193 mass as  $R_i$  and  $R_j$ , respectively (see Fig. 2). For example, in  
 194 the case shown in Fig. 2, the points lie on the particles' surfaces  
 195 and values  $R_i$  and  $R_j$  coincide with the particles' radii. Let us  
 196 introduce orthogonal unit vectors  $\mathbf{n}_i^1, \mathbf{n}_i^2, \mathbf{n}_i^3$  and  $\mathbf{n}_j^1, \mathbf{n}_j^2, \mathbf{n}_j^3$ ,  
 197 rigidly connected with particles  $i$  and  $j$ , respectively. The  
 198 lower indexes correspond to particles' numbers; the upper  
 199 indexes correspond to vectors' numbers. Assume that in the  
 200 undeformed state the following relations are satisfied:

$$\mathbf{n}_i^1 = -\mathbf{n}_j^1 = \mathbf{e}_{ij}, \quad \mathbf{n}_i^2 = \mathbf{n}_j^2, \quad \mathbf{n}_i^3 = \mathbf{n}_j^3. \quad (5)$$

201 Following the idea described in the previous paragraph, let  
 202 us represent the potential energy of the bond as a function  
 203 of vector  $\mathbf{D}_{ij} \stackrel{\text{def}}{=} \mathbf{r}_{ij} + R_j \mathbf{n}_j^1 - R_i \mathbf{n}_i^1$  and vectors  $\mathbf{n}_i^k, \mathbf{n}_j^m, k, m =$   
 204  $1, 2, 3$ . Vector  $\mathbf{D}_{ij}$  connects the "bonded" points with radius  
 205 vectors  $\mathbf{r}_i + R_i \mathbf{n}_i^1, \mathbf{r}_j + R_j \mathbf{n}_j^1$  (see Fig. 2). Let us consider the  
 206 following form for potential energy of the bond:

$$U = U_L(D_{ij}) + U_B(\mathbf{n}_i^1 \cdot \mathbf{n}_j^1, \mathbf{d}_{ij} \cdot \mathbf{n}_i^1, \mathbf{d}_{ji} \cdot \mathbf{n}_j^1) \\ + U_T(\{\mathbf{n}_i^k \cdot \mathbf{n}_j^k, \mathbf{d}_{ij} \cdot \mathbf{n}_i^k, \mathbf{d}_{ji} \cdot \mathbf{n}_j^k\}_{k=2,3}), \\ D_{ij} = |\mathbf{D}_{ij}|, \quad \mathbf{d}_{ij} = \mathbf{D}_{ij}/D_{ij}. \quad (6)$$

207 Note that potential energy (6) satisfies the objectivity prin-  
 208 ciple. That is, it is invariant with respect to rotation of the  
 209 system as a rigid body. Let us describe the relation between  
 210 functions  $U_L, U_B, U_T$  and different kinds of deformation of  
 211 the bond, shown in Fig. 3. Function  $U_L$  describes stretch-  
 212 ing/compression, function  $U_B$  describes bending and shear of

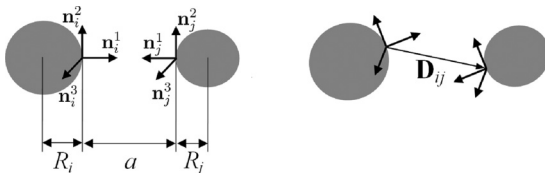


FIG. 2. Two bonded particles in the undeformed state (left) and deformed state (right). Here and below  $a$  is an equilibrium distance.

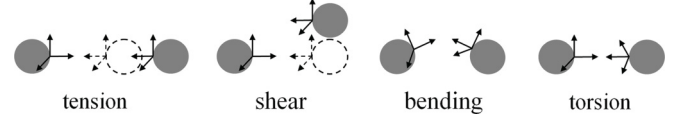


FIG. 3. Different kinds of deformation of the bond and corresponding change in vectors, connected with the particles. Dashed lines show the initial states of the particles.

the bond. Arguments  $\mathbf{d}_{ij} \cdot \mathbf{n}_i^1, \mathbf{d}_{ji} \cdot \mathbf{n}_j^1$  change in the case of 213  
 bending and shear. Argument  $\mathbf{n}_i^1 \cdot \mathbf{n}_j^1$  changes only in the case 214  
 of bending and is invariant with respect to shear. Function  $U_T$  215  
 changes in the case of both torsion and bending. The following 216  
 expressions for functions  $U_L, U_B, U_T$  from formula (6) are 217  
 proposed in the present paper: 218

$$U_L(s) = \frac{B_1}{2}(s - a)^2, \\ U_B(s_1, s_2, s_3) = -\frac{B_2}{2}s_1^2 - \frac{B_3}{2}(s_2^2 + s_3^2), \\ U_T(\{s_{1k}, s_{2k}, s_{3k}\}_{k=2,3}) = -\frac{B_4}{4} \sum_{k=2,3} (s_{1k} + s_{2k}s_{3k})^2 \\ \times (1 + s_{2k}^2)(1 + s_{3k}^2), \quad (7)$$

where  $a$  is an equilibrium length of the bond (see Fig. 2); 219  
 $B_m, m = 1, \dots, 4$ , are parameters of the model. Functions (7) 220  
 are the simplest with independent longitudinal, shear, bending, 221  
 and torsional stiffnesses (see Sec. IV A). Note that the number 222  
 of parameters of the V model is equal to the number of 223  
 bond stiffnesses. Further it is shown that the behavior of the 224  
 bond under small deformations can be described exactly by 225  
 fitting parameters of the model. For brittle materials, such as 226  
 rocks [4], it is sufficient as critical deformations are usually 227  
 small. On the other hand, it is shown below that the V model has 228  
 reasonable behavior at finite deformations (see Sec. VI). Thus, 229  
 very flexible structures can be considered as well. Also the V 230  
 model can be generalized for the nonlinear case, changing 231  
 expressions for  $U_L, U_B, U_T$  and introducing new parameters 232  
 into the potential. The generalization can be important, in 233  
 particular, for simulation of polymer bonds [7]. Note that 234  
 analogous generalization of existing models, such as the BPM 235  
 [4], is not so straightforward. 236

Let us derive expressions for force  $\mathbf{F}_{ij}$  and torque  $\mathbf{M}_{ij}$ . 237  
 Using formulas (3) and (7), one obtains 238

$$\mathbf{F}_{ij} = B_1(D_{ij} - a)\mathbf{d}_{ij} - \frac{B_3}{D_{ij}}\mathbf{d}_{ij} \cdot (\mathbf{n}_i^1 \tilde{\mathbf{n}}_i^1 + \mathbf{n}_j^1 \tilde{\mathbf{n}}_j^1) \\ + \frac{1}{D_{ij}} \sum_{k=2,3} \left( \frac{\partial U_T}{\partial s_{2k}} \tilde{\mathbf{n}}_i^k - \frac{\partial U_T}{\partial s_{3k}} \tilde{\mathbf{n}}_j^k \right), \\ \mathbf{M}_{ij} = R_i \mathbf{n}_i^1 \times \mathbf{F}_{ij} - \mathbf{n}_i^1 \cdot [B_2 \mathbf{n}_i^1 \mathbf{n}_i^1 + B_3 \mathbf{d}_{ij} \mathbf{d}_{ij}] \times \mathbf{n}_i^1 \\ + \sum_{k=2,3} \left( \frac{\partial U_T}{\partial s_{1k}} \mathbf{n}_j^k + \frac{\partial U_T}{\partial s_{2k}} \mathbf{d}_{ij} \right) \times \mathbf{n}_i^k. \quad (8)$$

Here and below  $\tilde{\mathbf{n}}_i^k = \mathbf{n}_i^k - \mathbf{n}_i^1 \cdot \mathbf{d}_{ij} \mathbf{d}_{ij}$ . The expressions for 239  
 partial derivatives  $\partial U_T / \partial s_{mk}, m = 1, 2, 3, k = 2, 3$  are the 240



241 following:

$$\begin{aligned} \frac{\partial U_T}{\partial s_{1k}} &= -\frac{B_4}{2}(s_{1k} + s_{2k}s_{3k})(1 + s_{2k}^2)(1 + s_{3k}^2), \\ \frac{\partial U_T}{\partial s_{2k}} &= -\frac{B_4}{2}(s_{1k} + s_{2k}s_{3k})(1 + s_{3k}^2) \\ &\quad \times (s_{3k} + s_{1k}s_{2k} + 2s_{3k}s_{2k}^2), \\ \frac{\partial U_T}{\partial s_{3k}} &= -\frac{B_4}{2}(s_{1k} + s_{2k}s_{3k})(1 + s_{2k}^2) \\ &\quad \times (s_{2k} + s_{1k}s_{3k} + 2s_{2k}s_{3k}^2), \quad k = 2, 3. \end{aligned} \quad (9)$$

242 Thus, formulas (8) and (9) are used for calculation of forces  
243 and torques, acting on the bonded particles. Note that in  
244 contrast to incremental procedure [4], the V model allows  
245 us to calculate forces and torques at every moment of time  
246 (time step) independently.

247 Note that the V model can be applied to both two- and  
248 three-dimensional problems. In two dimensions function  $U_T$   
249 describing torsion can be set equal to zero.

#### 250 IV. PARAMETER CALIBRATION

##### 251 A. Bond stiffnesses

252 Let us choose parameters of the V model  $B_m, m = 1, \dots, 4$   
253 in order to describe *any* given elastic properties of the bond  
254 in the case of small deformations exactly. Following the idea,  
255 proposed in Ref. [17], let us introduce stiffnesses of the bond.  
256 Consider the force  $\mathbf{F}_{ij}$  and torque

$$\mathbf{M} \stackrel{\text{def}}{=} \mathbf{M}_{ij} - (R_i \mathbf{n}_i^1 + \mathbf{D}_{ij}/2) \times \mathbf{F}_{ij}, \quad (10)$$

257 calculated with respect to the center of the bond, defined  
258 by vector  $\mathbf{r}_i + R_i \mathbf{n}_i^1 + \mathbf{D}_{ij}/2$ . According to the results of  
259 Ref. [17], under small deformations  $\mathbf{F}_{ij}$  and  $\mathbf{M}$  can be  
260 represented in the form

$$\begin{aligned} \mathbf{F}_{ij} &= \mathbf{A} \cdot (\mathbf{u}_j - \mathbf{u}_i - (R_i \boldsymbol{\varphi}_i + R_j \boldsymbol{\varphi}_j) \\ &\quad \times \mathbf{d}_{ij} + \frac{1}{2} \mathbf{D}_{ij} \times (\boldsymbol{\varphi}_i + \boldsymbol{\varphi}_j)), \\ \mathbf{M} &= \mathbf{G} \cdot (\boldsymbol{\varphi}_j - \boldsymbol{\varphi}_i), \end{aligned} \quad (11)$$

261 where  $\mathbf{A}$ ,  $\mathbf{G}$  are stiffness tensors;  $\mathbf{u}_i$ ,  $\boldsymbol{\varphi}_i$  are displacement and  
262 a vector indicating a small rotation of particle  $i$ . In the case  
263 of transversally symmetrical bonds, considered in the present  
264 paper, the stiffness tensors have form

$$\begin{aligned} \mathbf{A} &= c_A \mathbf{d}_{ij} \mathbf{d}_{ij} + c_D (\mathbf{E} - \mathbf{d}_{ij} \mathbf{d}_{ij}), \\ \mathbf{G} &= c_B (\mathbf{E} - \mathbf{d}_{ij} \mathbf{d}_{ij}) + c_T \mathbf{d}_{ij} \mathbf{d}_{ij}, \end{aligned} \quad (12)$$

265 where  $\mathbf{E}$  is a unit tensor. The values  $c_A, c_D, c_B, c_T$  are further  
266 referred to as longitudinal, shear, bending, and torsional  
267 stiffness, respectively. One can see from formulas (11)  
268 and (12) that the stiffnesses completely determine the behavior  
269 of the bond in the case of small deformations.

270 Let us derive the relations between parameters of potential  
271 (7) and bond stiffnesses. First consider the expression (8) for  
272 force  $\mathbf{F}_{ij}$  in the case of pure tension:

$$\mathbf{F}_{ij} = B_1 (D_{ij} - a) \mathbf{e}_{ij} = B_1 (|r_{ij} - R_i - R_j| - a) \mathbf{e}_{ij}. \quad (13)$$

273 Therefore, according to formula (11) longitudinal stiffness of  
274 the bond  $c_A$  is equal to  $B_1$ . Let us determine the relation

275 between shear stiffness  $c_D$  and parameter  $B_3$ . Consider the  
276 following deformation of the bond. Assume that position of  
277 particle  $i$  is fixed and particle  $j$  has a displacement  $u_j \mathbf{k}$ ,  
278 where  $\mathbf{k}$  is orthogonal to the line connecting particles in the  
279 undeformed state. Orientations of both particles are fixed. In  
280 this case the first formula from (11) has the form

$$\mathbf{F}_{ij} \cdot \mathbf{k} = c_D u_j. \quad (14)$$

281 Let us expand the expression (8) for  $\mathbf{F}_{ij}$  into a series, assuming  
282 that  $|u_j/a| \ll 1$  and neglecting the second order terms. In this  
283 case the projection of  $\mathbf{F}_{ij}$  on vector  $\mathbf{k}$  has form (14). Omitting  
284 the derivation let us present the final expression for  $c_D$ :

$$c_D = \frac{2B_3}{a^2}. \quad (15)$$

285 Let us obtain analogous relation for bending stiffness of  
286 the bond  $c_B$ . Assume that vector  $\mathbf{D}_{ij}$  remains fixed in the  
287 equilibrium state, while the particles are rotated by vectors  
288 of small turn  $\boldsymbol{\varphi}_i, \boldsymbol{\varphi}_j$ . In this case vectors  $\mathbf{n}_i^k, \mathbf{n}_j^m$  in the current  
289 (deformed) configuration can be calculated as follows:

$$\mathbf{n}_p^k \approx \mathbf{n}_p^k(0) + \boldsymbol{\varphi}_p \times \mathbf{n}_p^k(0), \quad k = 1, 2, 3, \quad p = i, j. \quad (16)$$

290 Here zero denotes initial configuration, for example,  $\mathbf{n}_i^1(0) =$   
291  $-\mathbf{n}_j^1(0) = \mathbf{e}_{ij}(0)$ . This deformation corresponds to bending the  
292 bond. Substituting (8) and (16) into (10) and leaving the first  
293 order terms only, one obtains

$$\mathbf{M} \approx \left[ \left( \frac{B_3}{2} + B_2 \right) (\mathbf{E} - \mathbf{d}_{ij} \mathbf{d}_{ij}) + B_4 \mathbf{d}_{ij} \mathbf{d}_{ij} \right] \cdot (\boldsymbol{\varphi}_j - \boldsymbol{\varphi}_i). \quad (17)$$

294 The expressions for bending stiffness  $c_B$  and torsional stiffness  
295  $c_T$  follows from the comparison of formula (17) with the  
296 second formula from (11). As a result the expressions relating  
297 the parameters of the V model to bond stiffnesses have the  
298 form

$$c_A = B_1, \quad c_D = \frac{2B_3}{a^2}, \quad c_B = \frac{B_3}{2} + B_2, \quad c_T = B_4. \quad (18)$$

299 It follows from formulas (18) that choosing parameters  
300  $B_m, m = 1, \dots, 4$  one can fit any values of the stiffnesses.  
301 Therefore, the linear elastic behavior of the bond can be  
302 described exactly. Note that no assumptions about bond's  
303 length/thickness ratio are made.

304 Thus, if stiffnesses of the bond are known, then the calcu-  
305 lation of V model parameters is straightforward. In principle,  
306 the stiffnesses can be measured, performing the experiments  
307 on tension, shear, bending, and torsion for the system of two  
308 bonded particles. In this case, formulas (18) are sufficient for  
309 calibration. However, if the body, for example, agglomerate  
310 [9], contains many bonds with different geometrical character-  
311 istics, then experimental calibration is practically impossible.  
312 Therefore, an additional model connecting the stiffnesses with  
313 geometrical and physical characteristics of the bond, such  
314 as bond length, shape, cross section area, elastic moduli of  
315 bonding material, etc., is required. Evidently the behavior of  
316 the bond strongly depends on bond's length/thickness ratio.  
317 Therefore, models used for calculation of the stiffnesses should

318 be different for the different ratios. Two procedures for long  
319 and short bonds are proposed below.

### 320 **B. Calibration for long bonds: The Bernoulli-Euler and** 321 **Timoshenko beam theories**

322 Assume that bonds are relatively long (length/thickness  
323 ratio is larger than unity). In this case, elastic beam, connecting  
324 particles, can be used as a model of the bond [15]. Comparison  
325 of the V model with the results of Bernoulli-Euler and  
326 Timoshenko beam theories [22] is used as a theoretical basis  
327 for calibration. Note that in contrast to Ref. [15], in the  
328 framework of the V model the bonds, connecting, for example,  
329 particle surfaces, can be considered. This fact is important for  
330 simulation of solids, composed of glued particles, for example,  
331 composites [7,10].

332 Let us derive the relation between parameters of the  
333 V model and massless Bernoulli-Euler beam connecting parti-  
334 cles (the beam connects points with radius vectors  $\mathbf{r}_i + R_i \mathbf{n}_i^1$   
335 and  $\mathbf{r}_j + R_j \mathbf{n}_j^1$ ). Assume that the beam has equilibrium length  
336  $a$ , constant cross section, and isotropic bending stiffness. The  
337 expressions for longitudinal, shear, bending, and torsional  
338 stiffnesses of a Bernoulli-Euler beam are derived in Ref. [21]:

$$c_A = \frac{EA}{a}, \quad c_D = \frac{12EJ}{a^3}, \quad c_B = \frac{EJ}{a}, \quad c_T = \frac{GJ_p}{a}, \quad (19)$$

339 where  $E, G, A, J$ , and  $J_p$  are Young's modulus, shear modulus,  
340 cross section area, moment of inertia, and polar moment of  
341 inertia of the cross section respectively. For example, for the  
342 beam with circular cross section

$$J = \frac{\pi d_b^4}{64}, \quad J_p = 2J, \quad A = \frac{\pi d_b^2}{4}, \quad (20)$$

343 where  $d_b$  is a diameter of the beam. Using formulas (18) and  
344 (19) one obtains the expressions, connecting parameters of the  
345 V model with characteristics of the beam

$$B_1 = \frac{EA}{a}, \quad B_2 = -\frac{2EJ}{a}, \quad B_3 = -3B_2, \quad B_4 = \frac{GJ_p}{a}. \quad (21)$$

346 Formula (21) can be used for calibration of the parameters  
347 in the case of long bonds. If the parameters are determined  
348 by formula (21), then under small deformations the V model  
349 is equivalent to a Bernoulli-Euler beam connecting particles.

350 Note that in this case values  $\tilde{B}_m \stackrel{\text{def}}{=} B_m a, m = 1, \dots, 4$ , do  
351 not depend on the equilibrium bond length  $a$ . Therefore,  
352  $\tilde{B}_m$  are the same for bonds with different length, but equal  
353 cross section and elastic properties. Using this fact one can  
354 reduce the number of parameters, stored in RAM, in computer  
355 simulations of systems with bonds of different length.

356 The Bernoulli-Euler model provides simple theoretical  
357 basis for calibration. However, if length and thickness of  
358 the bond are comparable, then this model is no longer  
359 applicable [22]. In this case more accurate models are required.  
360 Calibration using a Timoshenko model [22] is described below.

361 Consider a Timoshenko beam of length  $a$  and constant  
362 cross section with spherical inertia tensor. Let us derive the  
363 expressions, connecting parameters of the beam with its stiff-  
364 nesses. Longitudinal and torsional stiffnesses are determined  
365 by formulas (19). Without loss of generality the derivation of

expressions for shear and bending stiffnesses is carried out in  
the two dimensional case. Consider pure shear of the beam. The  
corresponding system of equilibrium equations and boundary  
conditions for the beam has the form [22]

$$w''(s) = \theta'(s), \quad \theta''(s) + \frac{\kappa A}{2J(1+\nu)}[w'(s) - \theta(s)] = 0, \quad (22)$$

$$w(0) = 0, \quad \theta(0) = 0, \quad w(a) = u_j, \quad \theta(a) = 0, \quad (23)$$

where  $\nu$  is Poisson's ratio of material of the bond;  $w(s)$  and  $\theta(s)$   
are the deflection and angle of rotation for the cross section  
with coordinate  $s$ ;  $\kappa$  is dimensionless shear coefficient [22].  
Shear coefficients for rods with different cross sections are  
derived, in particular, in Ref. [23].

Solving the system of partial differential equations (22)  
with boundary conditions (23) one obtains an expression for  
the magnitude of the shear force  $Q$ , acting in the beam, and  
shear stiffness:

$$Q = \kappa GA(w' - \theta) = c_D u_j, \quad c_D = \frac{12\kappa AEJ}{a[\kappa Aa^2 + 24J(1+\nu)]}. \quad (24)$$

Let us consider bending of the beam under the following  
boundary conditions:

$$w(0) = 0, \quad \theta(0) = \varphi_i, \quad w(a) = 0, \quad \theta(a) = \varphi_j. \quad (25)$$

Solving the system of equations (22) with boundary conditions  
(25) and calculating the magnitude of the torque  $M$ , acting in  
the middle of the beam, one obtains

$$M = EJ\theta'\left(\frac{a}{2}\right) = \frac{EJ}{a}(\varphi_j - \varphi_i). \quad (26)$$

Formula (26) gives the expression for the bending stiffness of  
the bond. Thus, the stiffnesses of a Timoshenko beam has form

$$c_A = \frac{EA}{a}, \quad c_D = \frac{12\kappa AEJ}{a[\kappa Aa^2 + 24J(1+\nu)]}, \quad (27)$$

$$c_B = \frac{EJ}{a}, \quad c_T = \frac{GJ_p}{a}.$$

Finally, using formulas (27) one obtains the relation between  
parameters of the V model and the Timoshenko beam:

$$B_1 = \frac{EA}{a}, \quad B_2 = -\frac{2EJ[\kappa Aa^2 - 12J(1+\nu)]}{a[\kappa Aa^2 + 24J(1+\nu)]}, \quad (28)$$

$$B_3 = \frac{6\kappa AEJa}{\kappa Aa^2 + 24J(1+\nu)}, \quad B_4 = \frac{GJ_p}{a}.$$

Note that in the limit  $\kappa \rightarrow \infty$  formulas (28) exactly coincide  
with analogous formulas (21), obtained using Bernoulli-Euler  
beam theory. If formula (28) is used for the calibration, then for  
small deformation the V model is equivalent to Timoshenko  
beam connecting particles.

### 393 **C. Calibration for short bonds**

394 Generally speaking, the approach for calibration described  
395 above is applicable for relatively long and thin bonds with  
396 length/thickness ratio larger than unity. In the case of short  
397 bonds, shown, for example, in Fig. 1, the models based

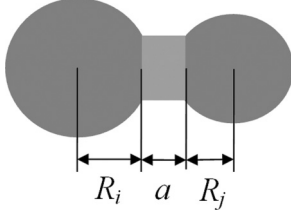


FIG. 4. Particles connected by a short cylinder.

398 on elasticity theory should be used for calibration. Let us  
 399 consider a simple qualitative model, based on elasticity theory.  
 400 Assume that particles are connected by a short cylinder with  
 401 equilibrium length  $a$  as is shown in Fig. 4. Note that, in general,  
 402 parameters  $R_i, R_j$  are not equal to particles' radii (the particles  
 403 can even be in contact with each other). Let us derive the  
 404 relations between the parameters of the bond and its stiffnesses.  
 405 Longitudinal stiffness  $c_A$  is, by definition, the proportionality  
 406 coefficient between force and elongation of the bond. In the  
 407 case of tension the force  $\mathbf{F}_{ij}$  is caused by the normal stress  $\sigma$ ,  
 408 acting in the bond. The following relation is satisfied:

$$\mathbf{F}_{ij} \cdot \mathbf{e}_{ij} = \int_{(A)} \sigma dA, \quad (29)$$

409 In the case of a short bond, rigidly attached to the particles,  
 410 the strain state of the bond is approximately uniaxial with  
 411 the strain equal to  $(u_j - u_i)/a$ , where  $u_i, u_j$  are particles'  
 412 displacements. Then the normal stress  $\sigma$  can be represented  
 413 using Hooke's law  $\sigma \approx (\lambda + 2\mu)(u_j - u_i)/a$ , where  $\lambda, \mu$  are  
 414 the Lamé coefficients for the bond. Substituting this formula  
 415 into Eq. (29) one obtains

$$\begin{aligned} \mathbf{F}_{ij} \cdot \mathbf{e}_{ij} &= \frac{(\lambda + 2\mu)A}{a} (u_j - u_i) \\ &= \frac{(1 - \nu)EA}{(1 + \nu)(1 - 2\nu)a} (u_j - u_i), \end{aligned} \quad (30)$$

416 Therefore, the longitudinal stiffness of the bond has the form

$$c_A = \frac{(1 - \nu)}{(1 + \nu)(1 - 2\nu)} \frac{EA}{a}. \quad (31)$$

417 One can see that longitudinal stiffness (31) differs from the  
 418 first formula from (27) by a factor of  $(1 - \nu)/[(1 + \nu)(1 - 2\nu)]$ .  
 419 Note that for nearly incompressible bonding materials  
 420 the difference is crucial.

421 Let us derive the expression for the shear stiffness  $c_D$ .  
 422 Consider pure shear of the bond. Assume that position of  
 423 particle  $i$  is fixed and particle  $j$  has a displacement  $u_j \mathbf{k}$ ,  
 424 where  $\mathbf{k}$  is orthogonal to the line connecting particles in the  
 425 undeformed state. Orientations of both particles are fixed. In  
 426 this case the force  $\mathbf{F}_{ij}$  is caused by shear stresses  $\tau$  acting  
 427 inside the bond. Integrating the stresses over the cross section  
 428 let us represent  $\mathbf{F}_{ij} \cdot \mathbf{k}$  in the following form:

$$\mathbf{F}_{ij} \cdot \mathbf{k} = \int_{(A)} \tau dA. \quad (32)$$

429 Assume that the stress distribution over the cross section  
 430 is uniform and  $\tau \approx Gu_j/a$ . Substituting this formula into  
 431 formula (32) and comparing the result with formula (14) one

obtains the following expression for shear stiffness:

$$c_D = \frac{GA}{a}. \quad (33)$$

One can see that the expression for shear stiffness (33) and the  
 second formula from (27), derived using Timoshenko beam  
 theory, are qualitatively different. However, it is notable that  
 the formulas coincide in the limit of vanishing length/thickness  
 ratio, if shear coefficient  $\kappa = 1$ . Analogous derivations for  
 bending and torsional stiffnesses of the bond lead to the  
 following results:

$$c_B = \frac{(1 - \nu)}{(1 + \nu)(1 - 2\nu)} \frac{EJ}{a}, \quad c_T = \frac{GJ_p}{a}. \quad (34)$$

Finally, using formulas (18) and (34) one obtains expressions,  
 connecting the parameters of the V model with bond charac-  
 teristics:

$$B_1 = \frac{(1 - \nu)EA}{(1 + \nu)(1 - 2\nu)a}, \quad B_2 = G \left[ \frac{2(1 - \nu)J}{1 - 2\nu} \frac{1}{a} - \frac{Aa}{4} \right], \quad (35)$$

$$B_3 = \frac{GAa}{2}, \quad B_4 = \frac{GJ_p}{a}.$$

Thus, in the case of short bonds formulas (35) can be used to  
 calibrate the V model.

## V. NUMERICAL IMPLEMENTATION OF THE V MODEL

Let us describe the numerical procedure for simulation  
 of solids using the V model. Consider the system of  $N$   
 particles, connected by bonds. Other types of interactions are  
 not considered in the present paragraph. The system of motion  
 equations has the classical form

$$m_i \ddot{\mathbf{r}}_i = \sum_{j \neq i} \mathbf{F}_{ij}, \quad \Theta_i \dot{\boldsymbol{\omega}}_i = \sum_{j \neq i} \mathbf{M}_{ij}, \quad (36)$$

where  $m_i, \Theta_i$  are the mass and the moment of inertia of the  
 particle (for simplicity, it is assumed that all particles have  
 spherical inertia tensor). If particles  $i$  and  $j$  are bonded, then  
 force  $\mathbf{F}_{ij}$  and torque  $\mathbf{M}_{ij}$ , caused by the bond, are calculated  
 using formulas (8). Otherwise, they are equal to zero. The  
 system (36) is solved together with the kinematic equations  
 connecting linear and angular velocities with positions and  
 orientations of the particles. For example, let us determine  
 the turn of particle  $i$  from initial orientation to current one by  
 rotational tensor  $\mathbf{P}_i$ . Then kinematic formulas are

$$\dot{\mathbf{r}}_i = \mathbf{v}_i, \quad \dot{\mathbf{P}}_i = \boldsymbol{\omega}_i \times \mathbf{P}_i. \quad (37)$$

Numerical integration of Eqs. (36) and (37) gives current  
 positions and orientations of the particles at every time step.

As was discussed, forces and torques between particles  $i$   
 and  $j$  are calculated using vectors  $\mathbf{n}_i^k, \mathbf{n}_j^k, k = 1, 2, 3$ , connected  
 with the particles. The vectors are introduced according to  
 formula (5) at moment  $t_*$ , when the bond is created, and  
 corotate with the particles. Consider the simplest approach  
 for calculation of their current coordinates. Let us introduce  
 the basis, consisting of orthogonal unit vectors  $\mathbf{x}_i^m, m = 1, 2, 3$ ,  
 rotating with particle  $i$ . Then current orientation of vectors  $\mathbf{x}_i^m$   
 is determined as follows:

$$\mathbf{x}_i^m(t) = \mathbf{P}_i(t) \cdot \mathbf{x}_i^m(0). \quad (38)$$

Let us use coordinates of vectors  $\mathbf{n}_i^k, k = 1, 2, 3$  in the comoving basis  $\mathbf{x}_i^m, m = 1, 2, 3$  for calculation of current orientation of the vectors  $\mathbf{n}_i^k, k = 1, 2, 3$ . Then at each time step vectors  $\mathbf{x}_i^m, m = 1, 2, 3$  are rotated using Eq. (38) and vectors  $\mathbf{n}_i^k$  are determined using their coordinates  $\mathbf{n}_i^k \cdot \mathbf{x}_i^m, m, k = 1, 2, 3$ , stored in RAM:

$$\mathbf{n}_i^k = \sum_{m=1}^3 (\mathbf{n}_i^k \cdot \mathbf{x}_i^m) \mathbf{x}_i^m. \quad (39)$$

Note that  $\mathbf{n}_i^k \cdot \mathbf{x}_i^m, k, m = 1, 2, 3$  does not depend on time and therefore can be calculated only at  $t = t_*$ . The described procedure allows us to avoid rotation of all vectors, connected with the particle, using Eq. (38).

Consider the calculation of forces and torques caused by the bonds. At every time step one should go over all the bonds and calculate corresponding forces and torques. Therefore in computer code, written in object-oriented programming language, it is convenient to introduce a class ‘‘Bond.’’ In general, the element of this class contains the following parameters: pointers to bonded particles, initial length of the bond  $a$ , parameters  $B_m, m = 1, \dots, 4$ , and coordinates of vectors  $\mathbf{n}_i^k, \mathbf{n}_j^k, k = 1, 2, 3$  in the comoving coordinate systems. For storage of the bonds it is also convenient to introduce a class for bond list. For example, in C++ language it can be implemented using `std::map`.

Thus, the algorithm for computer simulation using the V model is the following. At every time step, do the following.

- (1) Create new bonds if required. Calculate parameters of the bonds. Add created bonds to the list.
- (2) Check if the particles are bonded using list of the bonds. For each pair of bonded particles, get bond parameters and calculate current vectors  $\mathbf{n}_i^k, \mathbf{n}_j^k, k = 1, 2, 3$ , and length of the bond  $D_{ij}$ .
- (3) Calculate forces and torques between the particles using (8).
- (4) Calculate linear and angular velocities at the next time step.
- (5) Calculate positions and orientations of the particles and coordinates for vectors  $\mathbf{x}_i^k, k = 1, 2, 3$  at the next time step.

## VI. EXAMPLES

In general, using the V model one can simulate mechanical behavior of any solid consisting of (or represented by) bonded particles. However, accurate description of the bonds is especially important for computer simulation of thin rodlike [24] or shell-like granular structures [25]. The structures are widely used in the chemical industry and pharmaceuticals. In particular, the review on synthesis and application of shell-like polymer particles is given in Ref. [25]. In the present paper simulation of mechanical behavior of the simplest thin structures is carried out in order to test the applicability of the V model. Modeling of more complex and realistic structures is a subject for future work.

For simplicity, assume that all particles have the same mass  $m$  and radius  $R$ . The bonds connect particles’ centers and have circular cross section with diameter  $d_b$ . The Bernoulli-Euler model is used for the calibration. Let us represent all values via three dimensional parameters: equilibrium bond

length  $a$  [26], particle mass  $m$ , and longitudinal stiffness of the bond  $c_A$ . In computer code these parameters can be set equal to unity. All other parameters are represented via  $a, m, c_A$  and dimensionless values. In particular, the following dimensionless parameters are used:

$$\begin{aligned} \frac{Ea}{c_A} &= \frac{4}{\pi} \left( \frac{a}{d_b} \right)^2, & \frac{A}{a^2} &= \frac{\pi}{4} \left( \frac{d_b}{a} \right)^2, & \frac{J}{a^4} &= \frac{\pi}{64} \left( \frac{d_b}{a} \right)^4, \\ \frac{B_1}{c_A} &= 1, & \frac{B_2}{c_A a^2} &= -\frac{1}{8} \left( \frac{d_b}{a} \right)^2, & \frac{B_3}{c_A a^2} &= \frac{3}{8} \left( \frac{d_b}{a} \right)^2, \\ \frac{B_4}{c_A a^2} &= \frac{1}{16(1+\nu)} \left( \frac{d_b}{a} \right)^2. \end{aligned} \quad (40)$$

One can see that in this case the dimensionless parameters of the bond depends only on Poisson’s ratio  $\nu$  and the ratio  $d_b/a$ .

### A. Quasistatistical and dynamical buckling of a discrete beam

Consider the simplest thin structure, a notably straight discrete beam, directed along the  $x$  axis and consisting of  $N$  bonded particles. Assume that the bonds connect particles’ centers. First let us simulate quasistatistical buckling of the beam under compression using the following procedure. Initial velocities of the particles are randomly distributed in the circle with radius  $v_0$ . Initial angular velocities are set equal to zero. Every  $T_*$  time units the uniform deformation  $\varepsilon_*$  is applied to the discrete beam. After every deformation equations of particles motion (36) are integrated using leap-frog algorithm [3]. Translational degrees of freedom of the ends of the discrete beam remain fixed. The procedure is repeated until buckling. During the simulation compressive force acting in the beam is calculated and averaged with period  $T_*$ . The following values of the parameters are used:

$$\begin{aligned} N &= 10, & \frac{R}{a} &= 0.4, & \frac{\Theta}{ma^2} &= 64 \times 10^{-3}, & \frac{v_0}{v_*} &= 10^{-6}, \\ \frac{\Delta t}{T_0} &= 10^{-2}, & \frac{d_b}{a} &= 0.2, & \nu &= 0.2, & \frac{B_1}{c_A} &= 1, \\ \frac{B_2}{c_A a^2} &= -5 \times 10^{-3}, & \frac{B_3}{c_A a^2} &= 15 \times 10^{-3}, \\ \frac{B_4}{c_A a^2} &= 2.08 \times 10^{-3}, & \varepsilon_* &= -10^{-7}, & \frac{T_*}{T_0} &= 10, \end{aligned} \quad (41)$$

where  $\Theta$  is particle’s moment of inertia;  $\Delta t$  is a time step;  $T_0 = 2\pi\sqrt{m/c_A}$  is a period of small vibrations of one particle on the spring with stiffness  $c_A$ ;  $v_* = a\sqrt{c_A/m}$  is a velocity of long waves in one-dimensional chain, composed of particles with mass  $m$ , connected by springs with stiffness  $c_A$  and equilibrium length  $a$ .

As a result the following value of critical compressive force is obtained:  $f/(c_A a) = 3.19 \times 10^{-4}$ . The resulting value is only 4% higher than the static Euler critical force  $f_E/(c_A a) = \pi^2 E J / (c_A a^3) = 3.05 \times 10^{-4}$ . Note that in the framework of the Bernoulli-Euler model the critical force depends on the length and bending stiffness of the beam. Therefore, the bending stiffness of the discrete beam, composed of particles, within 4% accuracy coincides with the bending stiffness of the Bernoulli-Euler beam.

Consider the dynamical buckling of the same discrete beam. In addition to the V model, linear viscous forces



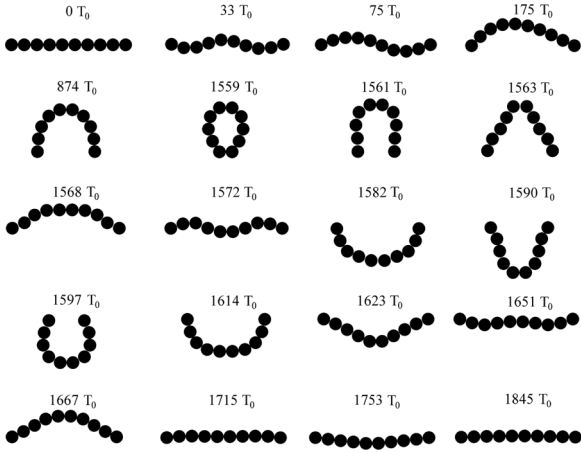


FIG. 5. Dynamical buckling of the discrete beam. Numbers in the figure are corresponding moments of time. Particles radii equal to  $0.5a$  are used for visualization.

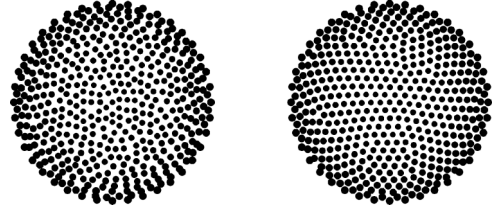


FIG. 6. The initial (left) and final (right) distributions of the particles on the half-sphere. Bottom view. Particles of radii  $0.125a$  are used for the visualization.

configuration. The other particles are generated randomly on the half sphere. The restriction that particles cannot be closer than  $0.4a$  to each other is used. Note that in this case  $a$  is a length scale of the problem. In general it is not equal to equilibrium bond length. The resulting random distribution of the particles is shown in Fig. 6 (left). Then the dynamics of translational motion of the particles interacting via repulsive force  $\mathbf{F}_{ij}^r$  only is simulated. The forces are calculated according to the following formula:

$$\mathbf{F}_{ij}^r = -f_0 \left( \frac{a}{r_{ij}} \right)^8 \mathbf{r}_{ij}. \quad (42)$$

The restriction  $r_i = R_c$ ,  $i = 1, \dots, N$  is applied during the simulation. The following values of the parameters are used for the simulation:

$$N = 458, \quad N_s = 15 \times 10^3, \quad \frac{v_0}{v_*} = 0, \quad \frac{\Delta t}{T_0} = 10^{-2}, \quad (43)$$

$$\frac{a_{\text{cut}}}{a} = 2.1, \quad \frac{f_0}{c_A} = 10^{-2}, \quad \frac{b}{b_0} = 26 \times 10^{-5},$$

where  $a_{\text{cut}}$  is a cutoff radius;  $N_s$  is a number of time steps. The initial and final distributions of the particles are shown in Fig. 6. One can see that the resulting distribution of the particles is much more uniform than the initial one.

After creation of the initial configuration the near-neighbor particles are bonded. For the sake of simplicity it is assumed that bonds connect particle centers. The equilibrium length for each bond is set equal to the distance between centers of the particles. Therefore, there is no residual stress in the initial state of the discrete shell. Also, it is assumed that parameters of the V model  $B_m, m = 1, \dots, 4$  are the same for all bonds. Dynamical buckling of the shell under the action of constant point force of magnitude  $f_s$  is considered. The force is applied along the axis of central symmetry of the shell until complete buckling occurs. In the given example the force vanishes at  $t/T_0 = 3000$ . Components of displacements of the boundary particles along the symmetry axis are set equal to zero. In order to avoid self-penetration of the shell contact Hertz forces  $\mathbf{F}_{ij}^H$  are introduced. The forces are calculated using the formula

$$\mathbf{F}_{ij}^H = \begin{cases} -\frac{c_H}{\sqrt{a}}(2R - r_{ij})^{\frac{3}{2}} \mathbf{e}_{ij}, & r_{ij} < 2R, \\ 0, & r_{ij} \geq 2R, \end{cases} \quad (44)$$

where  $c_H$  is a contact stiffness of the particle. Particle radius  $R$  is chosen so that  $2R$  is smaller than the minimum distance between particles in the initial configuration. The following

566 proportional to particles velocities are introduced. Denote  
 567 viscosity coefficient as  $b$ . Initial velocities of the particles  
 568 are randomly distributed inside the sphere with radius  $v_0$ . In  
 569 order to simplify visualization of the results  $z$  components of  
 570 the velocities for all particles are set equal to zero [27]. Initial  
 571 angular velocities are equal to zero. Let the ends of the beam  
 572 move toward each other with constant velocities  $v_e$  until the  
 573 distance between the ends becomes equal to  $a$  (see Fig. 5;  
 574  $t/T_0 = 1559$ ). Then  $x$  components of the velocities of the  
 575 beam ends are released and  $y$ -,  $z$ - components remain equal  
 576 to zero. The following values of dimensionless parameters  
 577 are used in addition to parameters (41):  $v_e/v_* = 10^{-3}$ ,  $b/b_0 =$   
 578  $26 \times 10^{-4}$ , where  $b_0 = 2\sqrt{mc_A}$  is a critical value of friction  
 579 for a two particle system. The motion of the discrete beam is  
 580 shown in Fig. 5. One can see the buckling and postbuckling  
 581 behavior of the discrete beam. At time  $t/T_0 = 33$  shape of  
 582 the discrete beam corresponds to the third buckling mode of  
 583 Bernoulli-Euler beam. The excitation of higher-order modes  
 584 of instability is typical for fast dynamical buckling. At the  
 585 moment  $t/T_0 = 1559$   $x$  components of velocities of the beam  
 586 ends are released and the beam performs strongly nonlinear  
 587 free vibrations, converging to its initial straight configuration  
 588 ( $t/T_0 > 1845$ ). Therefore, there is no plastic deformation.

589 Thus, the V model allows us to simulate large elastic  
 590 deformations of discrete rods including large displacements  
 591 and rotations of the particles. In the case of small deformations  
 592 considered above, the behavior of the discrete beam is in a good  
 593 agreement with Bernoulli-Euler beam theory.

## 594 B. Discrete half-spherical shell under the action of point force

595 Let us simulate the dynamical buckling of the discrete  
 596 half-spherical shell under the action of constant point force,  
 597 acting along the axis of central symmetry. The shell can be  
 598 considered as the simplest model of porous polymer particles,  
 599 described in the review [25]. Let us generate relatively uniform  
 600 distribution of particles on the half-sphere [28]. First, the circle  
 601 with radius  $R_c$  of the half-sphere is created. The number of  
 602 particles lying on the circle is calculated as the nearest integer  
 603 value to  $2\pi R_c/a$ . These particles are uniformly distributed  
 604 on the circle and remain fixed during creation of the initial



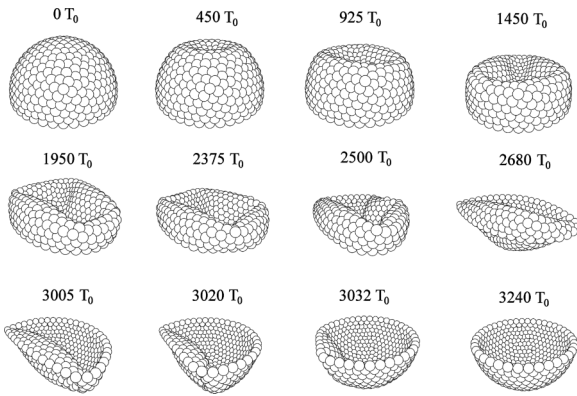


FIG. 7. Buckling of the discrete half-spherical shell under point force load. Particle radii equal  $0.5a$  are used for visualization.

640 values of the parameters are used for the simulation:

$$\begin{aligned}
 N &= 458, & \frac{R}{a} &= 0.35, & \frac{\Theta}{ma^2} &= 49 \times 10^{-3}, & \frac{v_0}{v_*} &= 10^{-6}, \\
 \frac{\Delta t}{T_0} &= 10^{-2}, & \frac{b}{b_0} &= 26 \times 10^{-4}, & \frac{d_b}{a} &= 0.2, & \nu &= 0.2, \\
 \frac{c_H}{c_A} &= 1, & \frac{f_s}{c_{AA}} &= 10^{-2}, & \frac{B_1}{c_A} &= 1, & \frac{B_2}{c_{AA}^2} &= -5 \times 10^{-3}, \\
 \frac{B_3}{c_{AA}^2} &= 15 \times 10^{-3}, & \frac{B_4}{c_{AA}^2} &= 2.08 \times 10^{-3}. & & & & (45)
 \end{aligned}$$

641 The results of the simulation are shown in Fig. 7. Buckling  
 642 and postbuckling behavior of the shell are presented. In the  
 643 places where the shell folds, the bonds undergo extremely large  
 644 rotations and deformation. For example, large deformations  
 645 occur at moment  $t/T_0 = 2680$  (see Fig. 7). However, large  
 646 deformations do not lead to any instability or other unphysical  
 647 behavior of the V model.

648 Thus, one can conclude that the V model is applicable for  
 649 computer simulation of discrete shells under large displacements,  
 650 rotations, and deformations.

## 651 VII. RESULTS AND DISCUSSIONS

652 In the present paper a new model for elastic bonds in  
 653 solids is proposed. Vectors rigidly connected with particles  
 654 are used for description of bond deformation. The expression  
 655 for potential energy of the bond as a function of the vectors is

656 proposed. Corresponding forces and torques acting between  
 657 bonded particles are calculated from a potential energy  
 658 function. This approach guarantees that the forces and torques  
 659 are conservative and the bonds are perfectly elastic. Dissipative  
 660 terms can also be added if required. Expressions connecting  
 661 parameters of the V model with longitudinal, shear, bending,  
 662 and torsional stiffnesses of the bond are derived in the case  
 663 of small deformations. It is shown that appropriate choices  
 664 of the parameters allow us to describe *any* values of all the  
 665 bond stiffnesses *exactly*. Two different calibration procedures  
 666 depending on bond length/thickness ratio are proposed. In the  
 667 case of beamlike bonds the comparison with Bernoulli-Euler  
 668 and Timoshenko beam theories are used for calibration. It  
 669 is shown that parameters of the V model can be chosen so  
 670 that under small deformations the bond is equivalent to either  
 671 Bernoulli-Euler or Timoshenko beam connecting particles.  
 672 Note that in the framework of the V model the bond may  
 673 connect any two points belonging to the particles and lying  
 674 on the line connecting particle centers in the initial state (in  
 675 particular, particles' centers or points lying on the surfaces).  
 676 The model for calibration in the case of short bonds is  
 677 proposed. In all the cases simple expressions, connecting  
 678 parameters of the V model with geometrical and mechanical  
 679 characteristics of the bond, are derived. Two examples of  
 680 computer simulations using the V model are given. The most  
 681 challenging structures, notably one layer thin discrete rods  
 682 and shells, are considered. Computer simulations of dynamical  
 683 buckling of the straight discrete beam and half-spherical shell  
 684 are carried out. It is shown that the V model is applicable for  
 685 description of large elastic deformations of solids composed  
 686 of bonded particles.

687 Simulation of fracture is not considered in the present paper.  
 688 However, the V model permits formulating fracture criteria for  
 689 the bond. For example, the criterion, proposed in Ref. [4], can  
 690 be directly implemented in the framework of the V model.

## 691 ACKNOWLEDGMENTS

692 The authors are deeply grateful to Michael Wolff, Sergiy  
 693 Antonyuk, Igor Berinskiy, and Anton Krivtsov for useful  
 694 discussions and motivation for this work. We also acknowledge  
 695 Nicoleta Preda for providing the image of nanocomposite,  
 696 shown in Fig. 1. We especially appreciate valuable suggestions  
 697 and criticism of Professor William Graham Hoover.

- [1] P. A. Cundall and O. D. L. Strack, *Geotechnique* **29**, 47 (1979).  
 [2] W. G. Hoover, in *Molecular Dynamics*, Lecture Notes in Physics, Vol. 258 (Springer, Berlin, 1986), p. 138.  
 [3] M. P. Allen and D. J. Tildesley, *Computer Simulation of Liquids*, (Clarendon Press, Oxford, 1987), p. 385.  
 [4] D. O. Potyondy and P. A. Cundall, *Int. J. Rock Mech. Min. Sc.* **41**, 1329 (2004).  
 [5] E. Schlangen and E. J. Garboczi, *Eng. Fract. Mech.* **57**, 2 (1997).  
 [6] D. Jauffrès, C. L. Martin, A. Lichtner, and R. K. Bordia, *Modell. Simul. Mater. Sci. Eng.* **20**, 045009 (2012).

- [7] M. F. H. Wolff, V. Salikov, S. Antonyuk, S. Heinrich, V. A. Kuzkin, and G. A. Schneider, in *Proceedings of XXIX International Summer School-Conference "Advanced Problems in Mechanics"*, St. Petersburg, 2011, edited by D. A. Indeytsev and M. A. Antimonov, p. 560.  
 [8] M. Khanal, W. Schubert, and J. Tomas, *Granular Matter* **7**, 83 (2005).  
 [9] S. Antonyuk, S. Palis, and S. Heinrich, *Powder Technol.* **206**, 88 (2011).  
 [10] N. Preda, E. Rusen, A. Musuc, M. Enculescu, E. Matei, B. Marculescu, V. Fruth, and I. Enculescu, *Mater. Res. Bull.* **45**, 1008 (2010).

- [11] Y. Wang, *Acta Geotech.* **4**, 117 (2009).
- [12] Contact interactions between particles are not considered in the present paper. However, they could be added independently, if required.
- [13] A. Refahi, J. A. Mohandesi, and B. Rezai, *J. S. African Inst. Mining Met.* **109**, 709 (2009).
- [14] S. Deng, R. Podgorney, and H. Huang, in *Proceedings of 36 Workshop on Geothermal Reservoir Engineering* (Curran Associates, Stanford, 2011).
- [15] S. Cole and D. Curry, in *Abstracts and Proceedings: WCPT6 - World Congress on Particle Technology, Nuremberg, Germany, 2010*, edited by Nurnberg Messe GmbH (Nuremberg, Germany, 2010).
- [16] E. A. Ivanova, A. M. Krivtsov, N. F. Morozov, and A. D. Firsova, *Doklady Physics* **48**, 8 (2003).
- [17] E. A. Ivanova, A. M. Krivtsov, and N. F. Morozov, *J. Appl. Math. Mech.* **71**, 543 (2007).
- [18] S. L. Price, A. J. Stone, and M. Alderton, *Mol. Phys.* **52**, 987 (1984).
- [19] I. E. Berinskii, E. A. Ivanova, A. M. Krivtsov, and N. F. Morozov, *Mech. Solids* **42**, 663 (2007).
- [20] V. A. Kuzkin and A. M. Krivtsov, *Dokl. Phys.* **56**, 527 (2011).
- [21] I. E. Berinsky, *NTV SPbSTU* **3**, 12 (2010) [in Russian].
- [22] S. Timoshenko, *Vibration Problems in Engineering* (Wolfenden Press, Garberville, CA, 2007), p. 480.
- [23] J. R. Hutchinson, *J. Appl. Mech.* **68**, 87 (2001).
- [24] Z. Grofa, M. Kohoutb, and F. Stepánek, *Chem. Eng. Sci.* **62**, 1418 (2007).
- [25] M. T. Gokmen and F. E. Du Prez, *Prog. Polym. Sci.* **37**, 365 (2012).
- [26] In the case of discrete shell considered below, the bonds have different lengths. Thus,  $a$  is a length scale of the problem.
- [27] Otherwise, the buckling is performed in several planes and the visualization is not so straightforward.
- [28] Note that the problem of setting the initial distribution of the particles problem is similar to the mesh-generation problem in the framework of, for example, the finite element method.